Supplementary Material

Laboratory-test results in reference-range values

The patient medical records showed multiple laboratory analyses resulting in normal-range values. Blood: 40 amino acids, acylcarnitines, very long chain fatty acids (C22, C24, C26), phytanic acid, pristatic acid, pipecolic acid, alpha-aminoadipic-delta-semialdehyde, alpha-glocosidase, palmitoyl thioesterase in leucocytes, folates, anti-endomysial antibody, anti-alpha-gliadin antibody. Urine: 34 amino acids (slight and non-reiterated increase in aspartate, proline and hydroxyproline), 20 organic acids (slight and non-reiterated increase in lactate and/or, methylmalonate, ethylmalonate, succinate, fumarate and 2-hydroxyglutarate), creatinine, mucopolysaccharides. Cerebrospinal fluid: 27 amino acids, 5-hydroxyindolacetic acid, homovanillic acid, 3,4-dihydroxyphenylacetic acid, 3-methoxy-4-hydroxphenylglycole, 3-O-methyl-Dopa, 5-hydroxytrytophan, 5-methylterahydrofolic acid, neopterin, biopterin. Fibroblasts: very long chain fatty acids, immunofluorescence detection of peroxisomes, dihydroxyacetonephosphate-acyltransferase activity.

WES and trio-WES analysis

Whole exome sequencing (WES) was performed using the Exome Capture Agilent V5+UTRs (71Mb) kit for library preparation and exome enrichment according to the manufacturer's instructions. Sequencing was conducted on the Illumina Genome Analyzer HiSeq2500 in paired-end mode, with a read length of 2x100bp, to generate at least 7 Gb per sample. Reads were filtered for sequencing quality and aligned to the human reference genome sequence (UCSC hg19, NCBI build 37.3) via the BWA program (1). Sequence variants were detected and annotated using the GATK toolkit (2), and the VEP program (3), respectively. The resulting variants were retained when the minor allele frequency was less than 0.005 in both the dbSNP146 database and in the ExAC database, or when variants were in genomic regions non-covered by those databases. No further cut-offs were applied permitting to retain also those variants that are commonly discarded, such us variants located in untranslated regions (UTRs), introns, promoters, synonymous variants, and missense variants that are not evolutionary conserved. The resulting sequence variants were then compared between the patient and his parents, using custom *Perl* scripts, under the following hypotheses of inheritance: dominant (*de novo* heterozygous variants) and recessive (homozygous variants and compound heterozygous variants). A visual inspection of the read alignments was performed to remove WES-mapping errors close to nucleotide repeats and other sequencing artifacts. The resulting mutated genes were prioritized for being suggestive of the disease using a deep screening of databases (publications, gene expression, protein location, metabolic function, phenotype of gene knockout mice and/or cell lines).

Minigene reporter construct assays

Minigene splicing reporter constructs were generated by PCR amplification of genomic DNA using Q5 proofreading DNA polymerase (New England Biolabs) and cloned into pCI-neo mammalian expression vector (Promega). Cells were cultured for 48 hours, and total RNA was purified using Ribozol RNA extraction reagent (AMRESCO) according to the manufacturer. Prior

to first strand synthesis, total RNA was subject to DNase I digestion with TURBO DNA-free kit (Ambion), and for each transfection 250 ng of total RNA were reverse transcribed using RevertAid first-strand cDNA synthesis kit (Thermo) with an oligo d(T)20 primer. The equivalent of 50 ng of starting RNA was used as template in each subsequent RT-PCR reaction in a total volume of 50 µL, with Maxima Hot Start Taq DNA polymerase (Thermo). Amplification was initiated by incubation for 5 min at 95 °C, followed by the appropriate number of cycles of 30 s at 94 °C, 30 s at 60 °C, and 20 s at 72 °C, with a final extension for 7 min at 72 °C. The linear range of amplification was determined independently for each PCR reaction. RT-PCR primers for minigene splice products were pCI-RT_F (5'-GTGTCCACTCCCAGTTCAATTACAG) and pCI_RT_R (5'- TGTCTGCTCGAAGCATTAACCC); RT-PCR primers for endogenous human beta actin were hACTIN_F (5'- ATGATGATATCGCCGCGCTC), and hACTIN_R (5'- CCACCATCACGCCCTGG). PCR products were separated on agarose gel (AMRESCO), visualized by GelRed nucleic acid stain (Biotium), and RT-PCR products were quantified using Fiji image processing analysis software (4). The identity of each RT-PCR product was confirmed by direct sequencing.

Experiments on yeast strains

S. cerevisiae strains used as model system of *SLC25A10* deficiency were wild-type (BY4742 MATα; leu2Δ0; ura3Δ0; his3Δ0; lys2Δ0; S288C yeast strain) and isogenic *ΔDIC1* (BY4742 MATα; ura3Δ0; leu2Δ0; his3Δ1; lys2Δ0; YLR348c::kanMX4) from EUROSCARF (EUROPEAN SACCHAROMYCES CEREVISIAE ARCHIVE FOR FUNCTIONAL ANALYSIS, http://www.euroscarf.de).

Yeast cells were pre-grown in YPD rich medium until exponential growth phase and inoculated at optical density of 0.05 at 600 nm in flasks with YP-Gly (1% yeast extract, 2% peptone, 2% glycerol) with and without 2.5 mM hydrogen peroxide. Cultures were grown at 30 °C. The growth rate was monitored by measuring the turbidity of the culture at 600 nm.

Petite frequency assays were conducted as reported (5). Briefly, yeast strains were grown 48 hours and 96 hours in YP-Gly rich medium at 30 °C in flasks. Selected respiratory competent yeast cells were plated on YPD agar medium and grown at 30 °C and 37 °C for 48 hours. The ratio between respiratory deficiency and respiratory competent yeast cells in each colony was measured by diluting and plating the single colony on YPD plate and performing Tetrazolium Chloride (TTC) assay. The final mixture for agar TTC overlay contains: 0.2% 2,3,5 -triphenyltetrazolium chloride (Sigma T8877), 0.067 M sodium phosphate buffer pH 7.0 and 1.5% bacto agar.

The relative amount of mitochondrial DNA (mtDNA) and nuclear DNA was determined by qPCR, as described (6). 20 ml of yeast cell culture grown in YP-Gly for 2 and 4 days at 30 °C were centrifuged at 3900xg and cells were either stored at −80 °C or immediately used for total DNA extraction using a "smash and grab" protocol (7). Briefly, cell pellets were re-suspended in 300 µl breaking buffer (2 % Triton X-100, 1 % SDS, 100 mM NaCl, 100 mM Tris-Cl pH 8.0, 1 mM EDTA), transferred in a 2 ml microcentrifuge tube with 300 µl glass beads (0.5 mm; BioSpec Products, Bartlesville, OK, USA) and 300 µl phenol/chloroform/isoamyl alcohol (25:25:1) solution. Cell disruption was carried out by means of a TissueLyser LT (Qiagen). The aqueous phase was transferred in a new tube and added with 1 ml cold ethanol. Ethanol was then discarded

by aspiration and the DNA pellet was resuspended in 100 µl water supplemented with RNase (0.1 µg/µl). DNA was quantified by absorbance at 260 nm. Real-time PCR was carried out using the QuantiTect® SYBR Green PCR Kit (Qiagen) and QuantStudio™ 6 Flex apparatus (Applied Biosystems) using the following primer pairs: for COX1: (F) 5′-CTACAGATACAGCATTTCCAAGA-3′ and (R) 5′- GTGCCTGAATAGATGATAATGGT-3′; for ACT1: (F) 5′-GTATGTGTAAAGCCGGTTTTG-3′ and (R) 5′-CATGATACCTTGGTGTCTTGG-3′ (Eurofins Genomics). 20 ng of total DNA (OD260/OD280 ≥ 1.9) were analyzed for each sample. The PCR protocol used was: 1 cycle at 95°C for 15 min; 35 cycles at 95 °C for 15 s, 58 °C for 30 s, 72 °C for 30 s; 1 cycle at 95 °C for 15 sec, 60 °C for 1 min, 95 °C for 15 sec. Four dilutions (10-fold) of the template DNA were used preliminarily to ensure measurements were within the linear range. For each strain analyzed, the relative copy number was calculated using the threshold cycle value (C_T). Values for C_T of the mitochondrial gene *COX1* and the nuclear gene *ACT1*, C_T (*COX1*) and C_T(*ACT1*), respectively, were calculated. The difference between these values (ΔC_T), i.e. C_T (*COX1*) - ΔC_T (*ACT1*), was determined and used to calculate $\Delta\Delta C_T$ between the ΔC_T value of each sample at 4 days of growth and the ΔC_T value of its control at 2 days of growth (ΔC_T4days - ΔC_T2days). The relative mtDNA copy number ($2^{-\Delta\Delta Ct}$) was calculated for each sample.

Supplementary Tables

Name	Genomic DNA (E:exon, I:intron)	Forward cloning primer	Reverse cloning primer	Fragment size
A	**E10**-I11-**E11**	ACAGTGGAATTCGGCGTTTTCCACTGCGC (*EcoRI*)	ACAGTGTCTAGAGGATGGCACTTTGATGCCAAAG (*XbaI*)	244
B	**E10**-I11-**E11**	ACAGTGGAATTCTCGGGCCTCTGGCCTTTTACAA (*EcoRI*)	ACAGTGTCTAGACCTCGATGGAAAGTGCTGGAAGAT (*XbaI*)	600 (A+387bp 3' UTR)
C	**E9**-I9-**E10**-I10-**E11**	ACAGTGCTCGAGGCCGCTGGTGACGAGC (*XhoI*)	ACAGTGTCTAGAGGATGGCACTTTGATGCCAAAG (*XbaI*)	2320
D	**E9**-I9-**E10**	ACAGTGCTCGAGGCCGCTGGTGACGAGC (*XhoI*)	ACAGTGTCTAGACTTGTAAAAGGCCAGAGGCCC (*XbaI*)	2131
E	**E8**-I8-**E9**-I9-**E10**	ACAGTGCTCGAGCTGTCCTGCTACGACCAGG (*XhoI*)	ACAGTGTCTAGACTTGTAAAAGGCCAGAGGCCC (*XbaI*)	2489

Supplementary table 1. *SLC25A10* genomic regions tested in minigene splicing reporter constructs.

The sequence of the restriction sites used for cloning is underlined.

Supplementary Figures

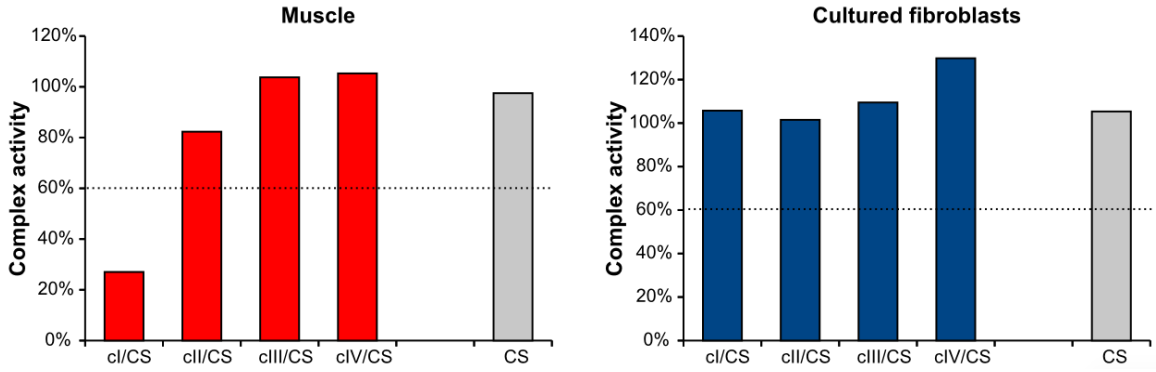

Supplementary figure 1. The patient presents respiratory complex I deficiency in skeletal muscle but not in cultured fibroblasts.

The enzymatic activity of each respiratory complex, normalized to citrate synthase activity (CS), is expressed as the percentage of the mean value in 100 normal control (8). cI: complex I, cII: complex II, cIII: complex III, cIV: complex IV. Specifically, complex I activity in skeletal muscle homogenates, normalized to citrate synthase activity, was 5.0, with control range 13-24, i.e. 27% of the mean control value. The activity of the other three complexes resulted within the control range. The activity of all the four complexes resulted within the control range in cultured fibroblasts.

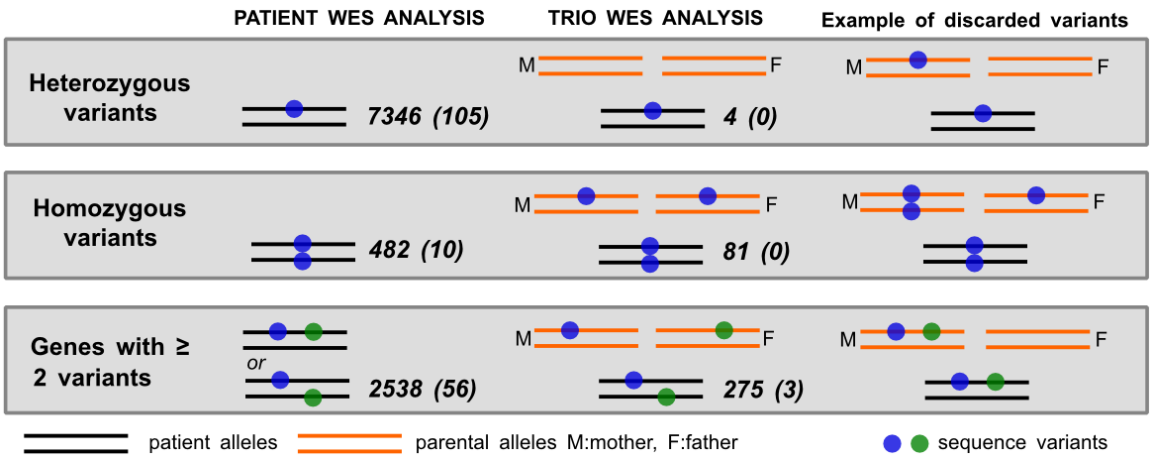

Supplementary figure 2. Trio-WES significantly reduces the total number of sequence variants respect to the patient-WES alone.

Each row refers to a class of DNA sequence variants. Numbers refer to sequence variants detected in the patient before (first column) or after (second column) having cut-off variants that are not compatible with a model of disease inheritance, according to the parental information furnished by trio-WES. The third column indicates examples of trio-based allele combinations that can be *a priori* cut-off by trio-WES analysis, without any further filtering criterion. Out of the three candidate genes encoding mitochondria-targeted proteins (numbers in brackets), *SLC25A10* was the only one compatible, for mutation frequency and function, with a disease phenotype. No other gene candidates than *SLC25A10* were found in the full gene dataset by deep analysis of the literature.

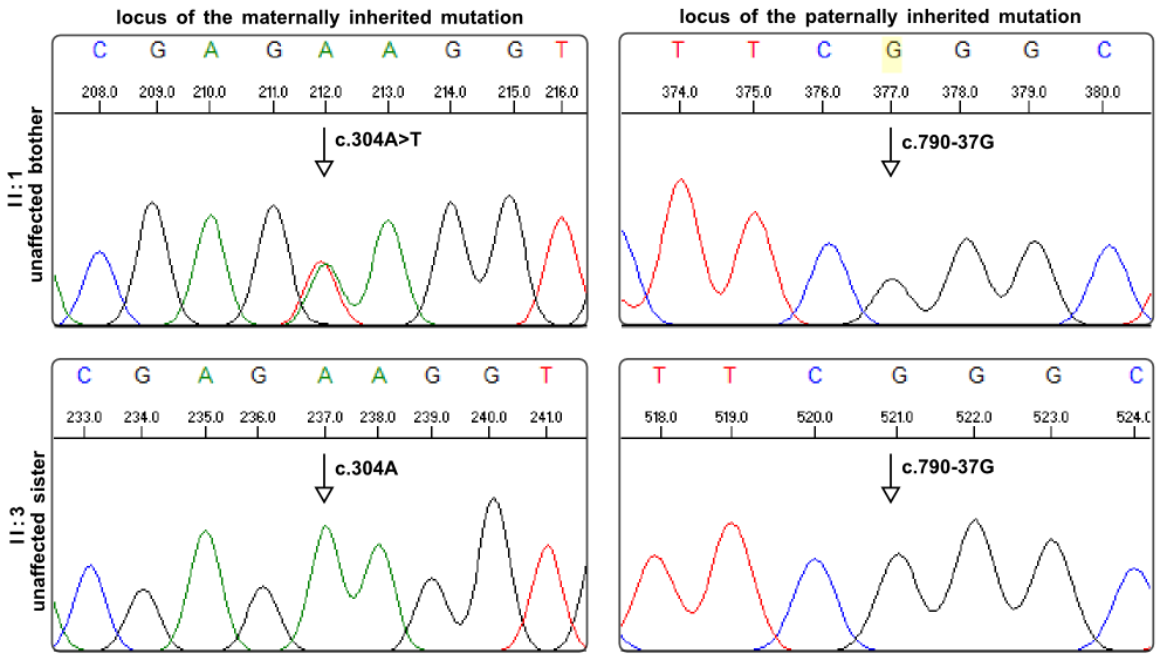

Supplementary figure 3. *SLC25A10* mutated alleles do not co-occur in the healthy brother and sister of the patient.

Sequences refer to genomic DNA of individuals II:1 and II:3, i.e. the unaffected brother and sister, respectively, of the patient. Individual II:1 only presents the maternally inherited mutation, while individual II:3 lacks both mutations. PCR primers are 5'-AGGGTGCAGCTCTAGATTTGTG-3' (forward) and 5'-ACCAGGGTCTCAGTGGCTTAT-3' (reverse) for the locus of the maternally inherited mutation, and 5'-ATCCCTGATTCTCATGGTTCTGT-3' (forward) and 5'-ACTCTTTGGAAGAACCTAGCGTGT-3' (reverse) for the locus of the paternally inherited mutation. The arrow indicates the nucleotide of interest, along-with its position in the reference sequence NM_001270888.

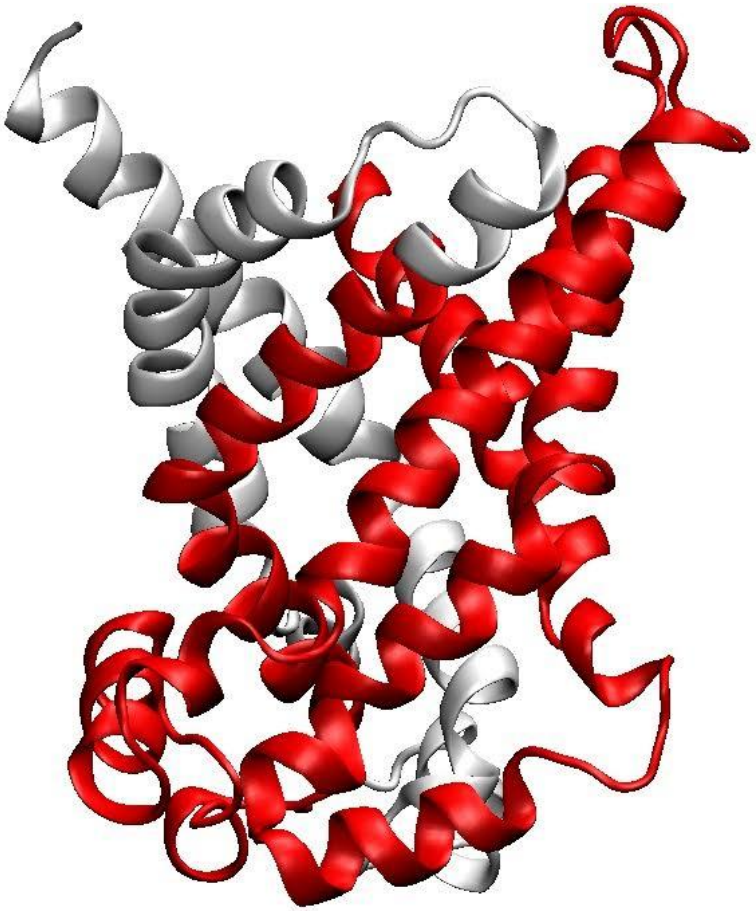

Supplementary figure 4. The maternally inherited allele encodes a prematurely truncated SLC25A10 protein.

The structure of the SLC25A10 protein is reported. The red color indicates the protein region that is not translated due to the premature stop codon mutation. The only translated protein sequence (gray) cannot exploit its carrier function, since the lack of four trans-membrane segments (out of six) hinders the formation of the full helix bundle required for the substrate translocation.

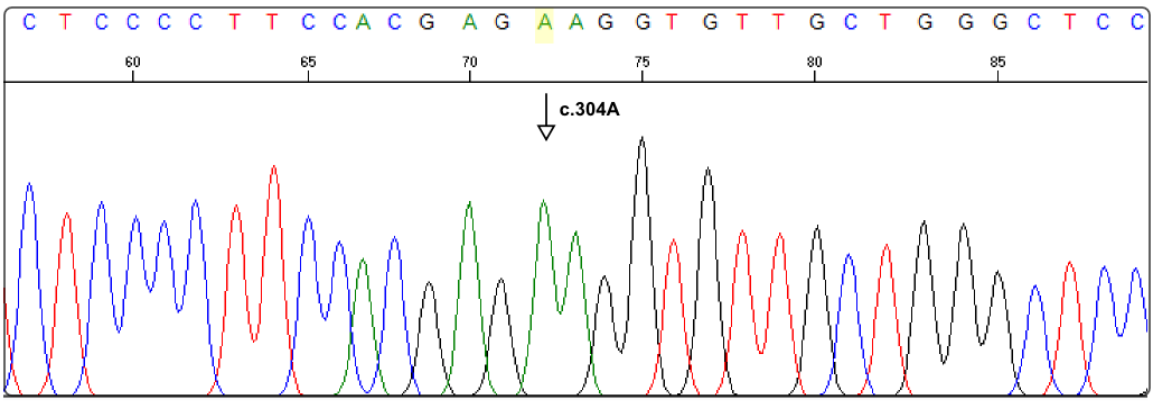

Supplementary figure 5. The endogenous *SLC25A10* mRNA of the patient corresponds to the paternally inherited allele only.

Sequence refers to the cDNA produced by RT-PCR from the RNA of the patient fibroblasts. The sequenced PCR fragment was generated by using primers F1 (5'-CAGACAGATGACCTACTCCCTGA-3') and R1 (5'-GACAAAGTGAGTGAAGATGTTGTCA-3'. The nucleotide of interest is indicated by an arrow, along with its position in the reference sequence NM_001270888. No PCR fragment was generated from the patient cDNA using primers F1 and R2 (5'-TTTGATGCCAAAGTTTTTGCGTAG-3').

NM_001270888 c.875C>T exon 9

Predicted signal	Prediction algorithm	cDNA Position
ESE Site Broken	1 - PESE Octamers from Zhang & Chasin	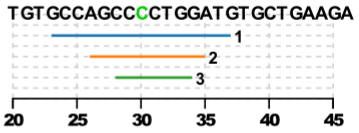
	2 - EIEs from Zhang et al.	
	3 - ESE-Finder - SF2/ASF(lg)	

NM_001270888 c.981-37G>A intron 10

Predicted signal	Prediction algorithm	cDNA Position
New ESE Site	1 - ESE-Finder - SRp40	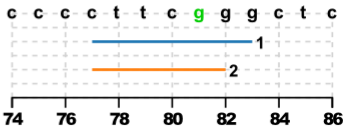
	2 - RESCUE ESE Hexamers	

Supplementary figure 6. The two paternally inherited mutations in *SLC25A10* are predicted to disrupt and create exon splicing enhancers, respectively.

The "Human Splicing Finder" (HSF) output is reported for each one of the two mutations located on the paternally inherited allele of the patient, i.e the synonymous mutation (upper panel) and the intronic mutation (lower panel). Only the most relevant effect on splicing is indicated per mutation, as reported in the HSF section "Interpreted result". Another predicted effect of the intronic mutation is the creation of a new acceptor splice site (gggccccttcAggc).

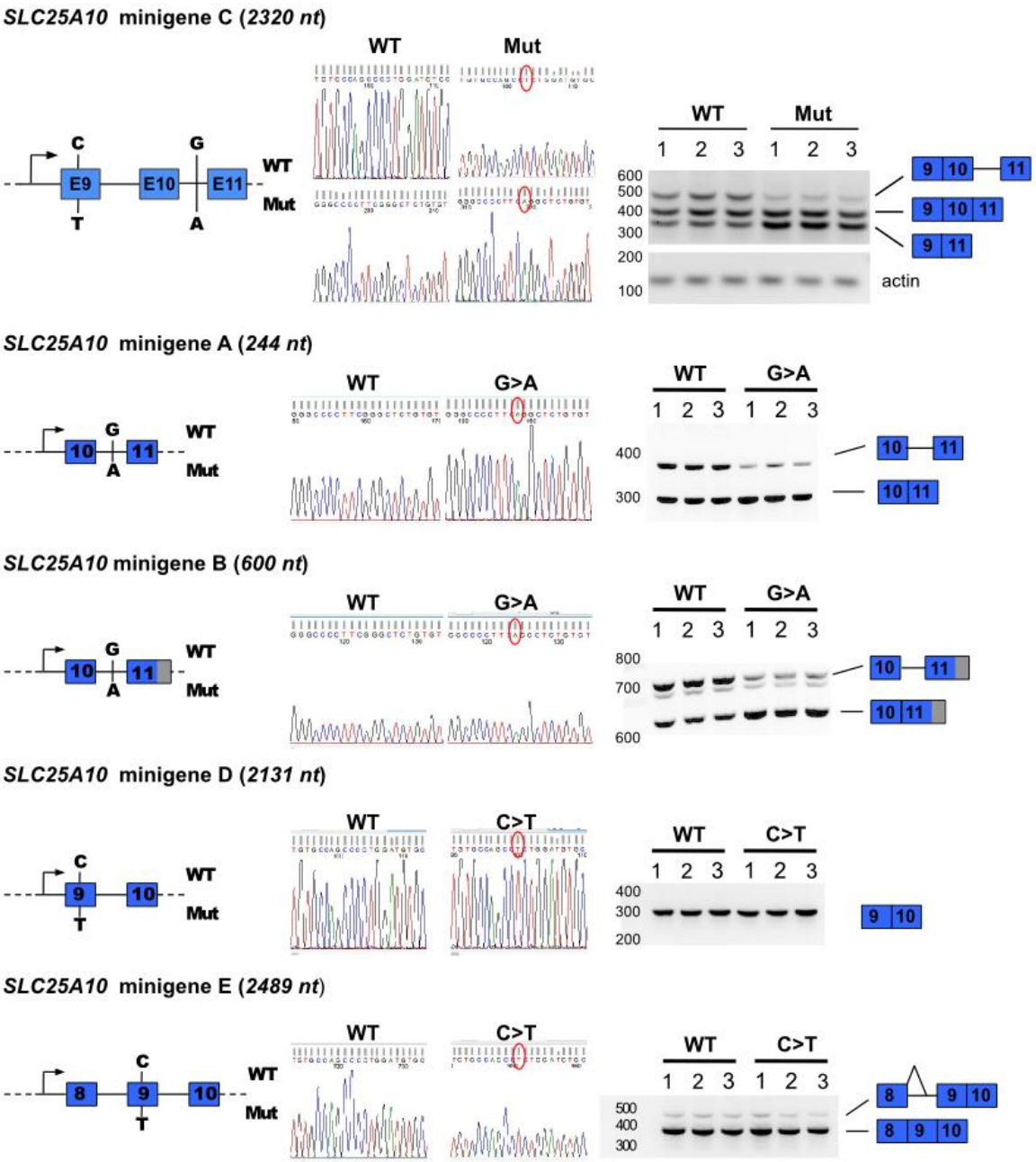

Supplementary figure 7. Effect of paternally inherited mutations on *SLC25A10* splicing in minigene constructs.

The structure of each minigene is reported (blue: coding sequence; gray: 3'UTR), along with the sequence identity of the cloned DNA (WT: wild-type; Mut: mutant). Electrophoresis gel analyses indicate cDNA PCR products obtained by expressing the cloned DNA into a mammalian vector. The intronic mutation alone (G>A), or together with the synonymous mutation (C>T), promotes the exclusion of intron 11, when compared to the WT nucleotide. No difference is observed in the two minigenes hosting the synonymous mutation (C>T) alone. Cells were transfected with each minigene in triplicate.

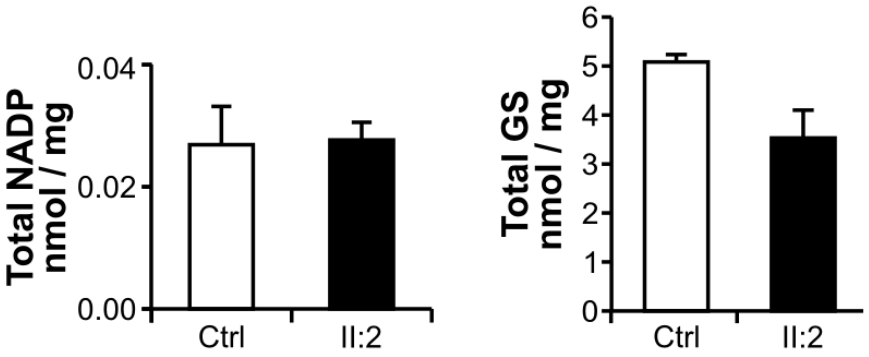

Supplementary figure 8. Total quantity of antioxidant molecules in patient and control fibroblasts.

Mass spectrometry quantification of total Nicotinamide Adenine Dinucleotide Phosphate (total NADP) and total glutathione (total GS) reported as the sum of quantities of the oxidized and reduced form, i.e. NADPH + $NADP^+$ and GSH + GSSG respectively, in cultured fibroblasts of patient (II:2) and control (Ctrl).

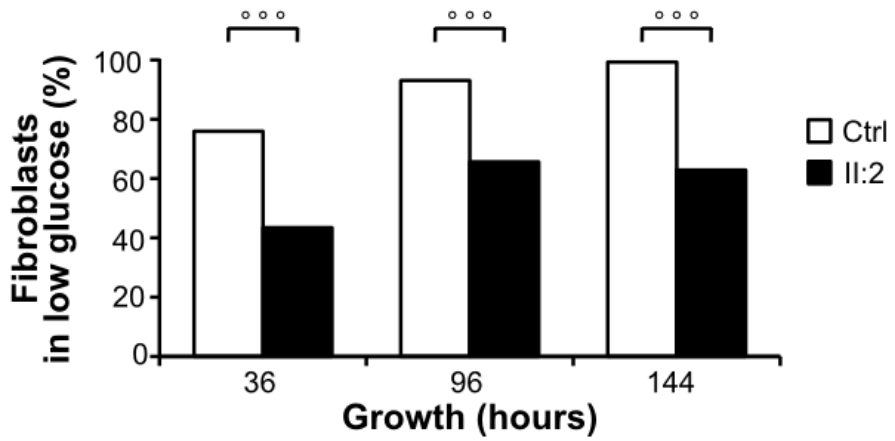

Supplementary figure 9. Growth defect of patient fibroblasts cultured in low glucose.

Patient (II:2) and control (Ctrl) fibroblasts were cultured in DMEM containing high-glucose concentration (4.5g/L) or low-glucose concentration (1 g/L) for 144 hours starting from 30,000 cells per well. The reported fibroblast percentage is the ratio between the cell count in low glucose and that in high glucose at each time point. °°°: chi-squared test p-value<0.05.

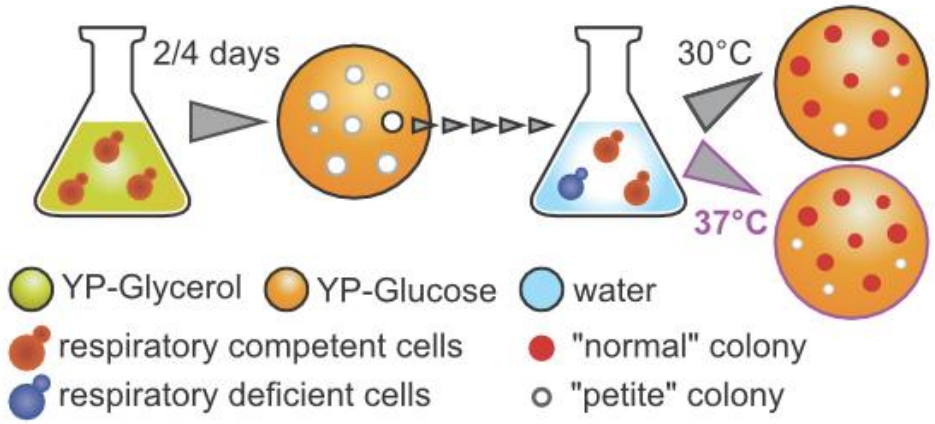

Supplementary figure 10. Overview of the "petite" frequency assay to measure the frequency of respiratory-deficient cells.

Yeast cells were grown in a rich medium containing glycerol, a non-fermentable carbon source, to kill respiratory-deficient cells and to stimulate mitochondrial biogenesis (for 2 or 4 days). An aliquot of the cell culture was diluted and plated on glucose to obtain colonies founded by a single respiratory-proficient cell, whose daughter cells, grown on glucose, may loose respiratory competency. To quantify the percentage of respiratory-deficient daughter cells, each well-formed colony was picked, resuspended in water, plated on glucose and overlaid with tetrazolium salt Respiratory-deficient cells appears as small and white ("petite") colonies, since they cannot reduce tetrazolium salts. All steps were conducted at 30°C, while the final step also at 37°C.

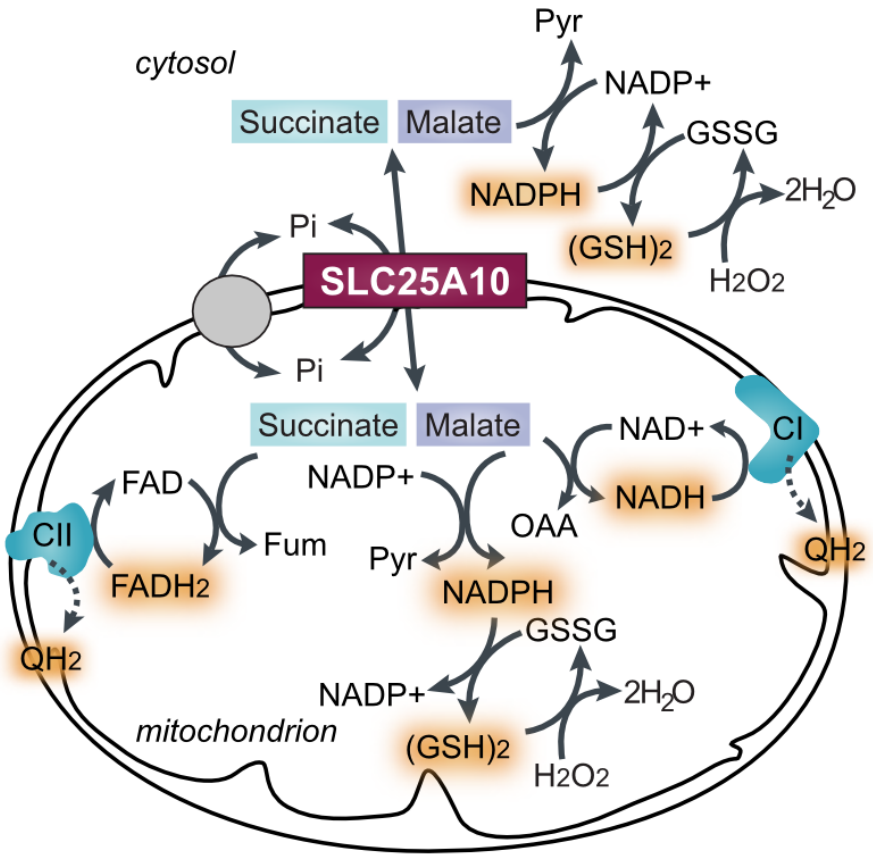

Supplementary figure 11. SLC25A10-mediated transport of reducing equivalents between cytosol and mitochondria.

SLC25A10 promotes the transfer of reducing equivalents (orange) across the inner mitochondrial membrane by transporting malate or succinate in exchange with phosphate (Pi). In both mitochondria and cytosol, reducing equivalents are transferred from malate to NADP+ by malic enzyme to form NADPH, and from NADPH to oxidized glutathione (GSSG) by glutathione reductase to form reduced glutathione (GSH). GSH is oxidized by glutathione peroxidase to convert hydrogen peroxide (H_2O_2) into water. In addition, mitochondrial malate- and succinate-carried reducing equivalents are transferred to NAD+ and FAD by malate dehydrogenase and succinate dehydrogenase, respectively. The reducing equivalents of the cofactors NADH and $FADH_2$ enter the respiratory chain and are transferred to ubiquinone, forming ubiquinol (QH_2), by complex I (CI) and by complex II (CII), respectively. Pyr: pyruvate; OAA: oxalacetate; Fum: fumarate.

Supplementary References

1. Li, H. and Durbin, R. (2009) Fast and accurate short read alignment with Burrows-Wheeler transform. *Bioinformatics*, **25**, 1754–1760.

2. McKenna, A., Aaron, M., Banks, E., Sivachenko, A., Cibulskis, K., Kernytsky, A., Garimella, K., Altshuler, D., Gabriel, S., Daly, M., *et al.* (2009) The Genome Analysis Toolkit: A MapReduce framework for analyzing next-generation DNA sequencing data. *Genome Res.*, **20**, 254–260.

3. McLaren, W., Pritchard, B., Rios, D., Chen, Y., Flicek, P. and Cunningham, F. (2010) Deriving the consequences of genomic variants with the Ensembl API and SNP Effect Predictor. *Bioinformatics*, **26**, 2069–2070.

4. Schindelin, J., Arganda-Carreras ,I., Frise, E., Kaynig, V., Longair, M., Pietzsch, T., Preibisch, S., Rueden, C., Saalfeld, S., Schmid, B., *et al.* (2012) Fiji: an open-source platform for biological-image analysis. *Nat. Methods*, **9**, 676–82.

5. Hess, D.C., Myers, C.L., Huttenhower, C., Hibbs, M.A., Hayes, A.P., Paw ,J., Clore, J.J., Mendoza, R.M., Luis, B.S., Nislow, C., *et al.* (2009) Computationally Driven , Quantitative Experiments Discover Genes Required for Mitochondrial Biogenesis. *PLoS Genet.*, **5**, e1000407.

6. Taylor, S.D., Zhang, H., Heaton, J.S., Rodeheffer, M.S., Lebedeva, M.A., O'Rourke, T.W., Siede, W. and Shadel, G.S. (2005) The Conserved Mec1/Rad53 Nuclear Checkpoint Pathway Regulates Mitochondrial DNA Copy Number in Saccharomyces cerevisiae. *Mol. Biol. Cell*, **16**, 3010–3018.

7. Hoffman, C.S. and Winston, F. (1987) A ten-minute DNA preparation from yeast efficiently releases autonomous plasmids for transformaion of Escherichia coli. *Gene*, **57**, 267–272.

8. Bugiani, M., Invernizzi, F., Alberio, S., Briem, E., Lamantea, E., Carrara, F., Moroni, I., Farina, L., Spada, M., Donati, M.A., *et al.* (2004) Clinical and molecular findings in children with complex I deficiency. *Biochim. Biophys. Acta*, **1659**, 136–147.